Stability of a Continuous-Time State Variable Filter with Op-amp and OTA-C Integrators

Tim Bakken, University of Southern California
John Choma, Jr., University of Southern California

Abstract

The stability of a continuous-time state variable filter is analyzed using the Routh-Hurwitz criterion. This criterion assesses stability by indicating the number of poles that lie in the right-half plane. The filter is examined separately with integrators implemented with an op-amp and an OTA-C. Both amplifier types are characterized by a dominant-pole frequency response, and the stability of each implementation is compared. HSPICE simulations confirm the theoretical analyses, which indicate that the gain-bandwidth product of the op-amps and the bandwidth of the OTAs must be much larger than the desired frequency of operation to ensure stability. Since the analyses assume a dominant-pole response, all higher-order poles of the actual amplifier must also be much greater than the unity-gain frequency to minimize excess phase.

I. Introduction

Several classes of continuous-time active filters, including state variable structures, rely on integrators to provide the required poles and zeros [1]. Traditional integrator architectures use voltage-mode operational amplifiers (op-amps) with capacitive feedback to integrate the applied voltage signal. However, the limited frequency response of conventional op-amps, as well as the dominant-pole open-loop constraints required for stable closed-loop operation, restricts the operation of the resultant filter to frequencies below 100 kHz [2]. Since modern communication systems require the processing of signals near 1 GHz, research into other integrator topologies, such as the operational transconductance amplifier-capacitor (OTA-C), has increased in recent years [3]-[5].

To assess the performance of each implementation, this paper compares the stability of a continuous-time state variable filter implemented with op-amp integrators to the stability of the same filter implemented with OTA-C integrators. In each case, the frequency response of the basic amplifier is characterized by a dominant pole. The filter, shown in Fig. 1, requires two integrators and simultaneously offers low-pass, bandpass, and high-pass output nodes [1]. In sections III and IV, the bandpass transfer function of each implementation is found, and its stability analyzed using the Routh-Hurwitz criterion. This criterion assesses the stability of the resulting fourth-order transfer functions, and provides design equations that relate the stability of the filter to circuit parameters. HSPICE simulations confirm theoretical results.

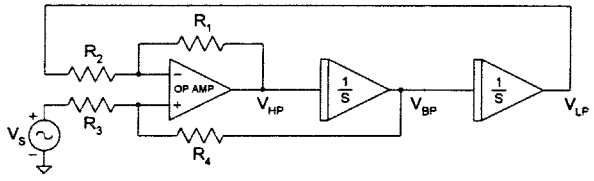

Figure 1. State variable filter

II. Circuit transformation

For analytical simplicity the filter is transformed in Fig. 2 by replacing the op-amp and feedback resistors with controlled sources.

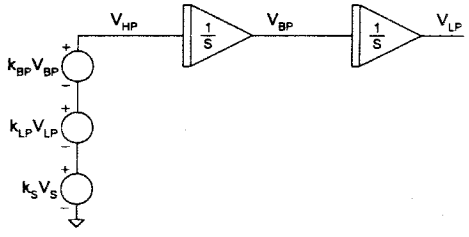

Figure 2. Modified state variable filter

The coefficients of these sources are

$$k_{LP} = -\frac{R_1}{R_2} \tag{1}$$

$$k_S = \left(1+\frac{R_1}{R_2}\right)\left(\frac{R_4}{R_3+R_4}\right) \tag{2}$$

$$k_{BP} = \left(1+\frac{R_1}{R_2}\right)\left(\frac{R_3}{R_3+R_4}\right) \tag{3}$$

Assuming both integrators in the filter of Fig. 2 are ideal, the quality factor (Q) and the magnitude at the center

0-8186-8409-7/98 $10.00

frequency of the bandpass output (H_{BP}) can be shown to be

$$Q = \frac{\sqrt{-k_{LP}}}{k_{BP}} \tag{4}$$

and

$$H_{BP} = -\frac{k_S}{k_{BP}} \tag{5}$$

The center frequency depends on the transfer function of the integrators, which is different for the op-amp and OTA-C implementations. Expressions for the center frequency are given in sections III and IV. The filter of Fig. 2 containing k_{LP}, k_S, and k_{BP} is used to analyze and simulate both integrator implementations, where k_S = -1.9 and k_{LP} = -1. The third coefficient, k_{BP}, is varied to select the desired Q of the filter.

III. Op-amp realization

Fig. 3 depicts a model of the voltage-feedback op-amp integrator used to implement the filter of Fig. 2. The frequency response of the open-loop op-amp gain is characterized by a dominant pole created by R_{POLE} and C_{POLE}. The controlled source, A_2, buffers the output, while R_{INT} and C_{INT} comprise the integrating elements. Although R_{IN} and R_{OUT} are included in the HSPICE simulations of the filter, these elements are assumed ideal (i.e., $R_{IN} = \infty$ and $R_{OUT} = 0$) in hand calculations.

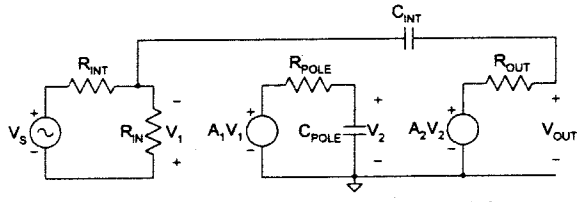

Figure 3. Op-amp integrator model

A. Theoretical analysis

Supplanting each integrator in the filter of Fig. 2 with the model of Fig. 3 (assuming R_{OUT} = 0) results in the fourth-order circuit depicted in Fig. 4. Analyses show that the bandpass transfer function is

$$\frac{V_{BP}}{V_S} = \frac{k_s A_{11} X_{21}}{X_{11} X_{21} - k_{LP} A_{11} A_{21} + k_{BP} A_{11} X_{21}} \tag{6}$$

where

$$X_{11} = 1 + s\left[T_{11} + T_{12}\left(1 + A_{11}\right)\right] + s^2 T_{11} T_{12} \tag{7}$$

$$X_{21} = 1 + s\left[T_{21} + T_{22}\left(1 + A_{21}\right)\right] + s^2 T_{21} T_{22} \tag{8}$$

and $T_{ij} = R_{ij}C_{ij}$, for i = 1, 2 and j = 1, 2.

The bandwidth (BW) of each op-amp and center frequency (ω_n) of the filter are

$$BW = \frac{1}{R_{POLE} C_{POLE}} \tag{9}$$

where $R_{POLE} = R_{11} = R_{21}$ and $C_{POLE} = C_{11} = C_{21}$, and

$$\omega_n = \frac{\sqrt{-k_{LP}}}{R_{\omega n} C_{\omega n}} \tag{10}$$

where $R_{\omega n} = R_{12} = R_{22}$ and $C_{\omega n} = C_{12} = C_{22}$.

The stability of the bandpass transfer function is assessed by analyzing the pole locations. Although finding the exact pole locations is mathematically cumbersome, applying the Routh-Hurwitz criterion to the characteristic polynomial of the circuit indicates the number of poles that lie in the right half of the complex frequency plane. Applying the Routh-Hurwitz criterion directly to the denominator of (6) is analytically impractical, so three approximations are made based on the relative values of circuit parameters. Typical values are selected for the open-loop gain (A_0) and bandwidth of the op-amps to be A_0 = 200 kV/V and BW = 2.5 kHz. Using typical values of Q, the three assumptions, $A_0 >> 1$, $A_0 >> 2Q$, and $A_0 >> 1/Q$, are easily satisfied.

Under these conditions, and assuming the two integrators are matched such that $A_{11} = A_{21}$, $T_{11} = T_{21}$, and $T_{12} = T_{22}$, the characteristic polynomial of (6) becomes

$$s^4 a_4 + s^3 a_3 + s^2 a_2 + s a_1 + a_0 \tag{11}$$

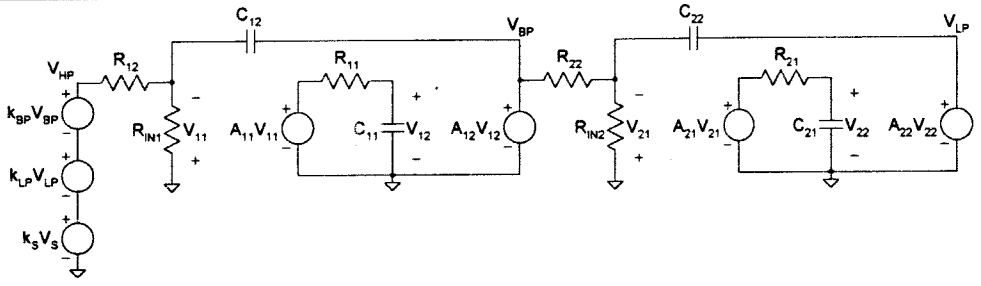

Figure 4. State variable filter with op-amp integrators

where

$$a_4 = T_{11}^{\ 2} T_{12}^{\ 2} \tag{12}$$

$$a_3 = 2T_{11}T_{12}\left(T_{11} + A_{11}T_{12}\right) \tag{13}$$

$$a_2 = 2A_{11}T_{11}T_{12} + T_{11}^{\ 2} + A_{11}^{\ 2}T_{12}^{\ 2} + k_{BP}A_{11}T_{11}T_{12} \tag{14}$$

$$a_1 = k_{BP}A_{11}\left(T_{11} + A_{11}T_{12}\right) \tag{15}$$

$$a_0 = A_{11}^{\ 2} \tag{16}$$

The Routh-Hurwitz criterion states that the number of algebraic sign changes in the first column of the Routhian array is numerically equal to the number of right-half plane zeros of the polynomial in question [6]. For a fourth-order polynomial in the form of (11), the Routhian array is

$$\begin{bmatrix} s^4 & a_4 & a_2 & a_0 \\ s^3 & a_3 & a_1 & 0 \\ s^2 & c_1 & c_2 & 0 \\ s^1 & d_1 & 0 & 0 \\ s^0 & e_1 & 0 & 0 \end{bmatrix} \tag{17}$$

where c_1, c_2, d_1, and e_1 are defined by (18) through (21). Routhian array first column elements a_4, a_3, c_1, and e_1 are positive, so stability is ensured if d_1 is also positive. Element d_1 is positive for

$$\frac{2A_0BW}{\omega_n} + \frac{2\omega_n}{A_0BW} > 4Q - \frac{1}{Q} - 4 \tag{22}$$

With $A_0BW >> \omega_n$ and $Q >> 1$, (22) may be approximated as

$$A_0BW > 2Q\omega_n \tag{23}$$

B. Simulation results

For low values of Q, the filter is stable to higher frequencies where the assumption, $A_0BW >> \omega_n$, is no longer valid. Under such conditions, the more precise inequality of (22) is required to accurately describe the stability of the filter. For $Q \leq 2.12$, for example, (22) correctly predicts the filter is stable for all frequencies, while (23) predicts stability for all frequencies only for $Q = 0$. HSPICE simulations verify the accuracy of both (22) and (23), however, as (23) is more straightforward, it will be used to present simulation results.

To ensure stability, (23) indicates that the gain-bandwidth product (*GBP*), A_0BW, of the op-amps used in the state variable filter of Fig. 1 must be at least twice the product of the quality factor, Q, and the desired center frequency, ω_n. Moving the poles farther from the imaginary axis to eliminate peaking at the center frequency requires the *GBP* of the op-amps to be even larger – typically 10 times larger – than $2Q\omega_n$. HSPICE simulations verify this claim, as indicated by the results in Table 1 on the following page. In all simulations, Q, and the center frequency magnitude, H_{BP}, are designed to be 10 and 19, respectively. Since $Q >> 1$, the filter will become unstable at lower frequencies where the assumption, $A_0BW >> \omega_n$, is valid. Therefore, (23) may be used to predict stability.

In the first simulation of Table 1, (23) is not satisfied with the chosen values of Q, ω_n, and *GBP*. Accordingly, the filter is unstable and has poles in the right half of the complex frequency plane. The next three simulations use an increasingly larger *GBP*, and the resulting H_{BP} decreases as the poles move into the left-half plane and farther from the imaginary axis. The fifth simulation doubles the original *GBP* from 500 MHz to 1 GHz, causing the frequency of oscillation to double from 28 to 56 MHz.

The first five simulations use the *BW* to change the *GBP*, so the last simulation changes the *GBP* with the gain, A_0. In this case, the original *GBP* is multiplied by ten, forcing the resulting oscillation frequency to a value ten times the original. The simulated circuit, therefore, behaves exactly as (23) predicts.

$$c_1 = \frac{a_3a_2 - a_4a_1}{a_3} = \frac{4A_{11}T_{11}T_{12} + 2T_{11}^{\ 2} + 2A_{11}^{\ 2}T_{12}^{\ 2} + k_{BP}A_{11}T_{11}T_{12}}{2} \tag{18}$$

$$c_2 = a_0 = A_{11}^{\ 2} \tag{19}$$

$$d_1 = \frac{c_1a_1 - a_3c_2}{c_1} = \frac{\left(4k_{BP}A_{11}^{\ 2}T_{11}T_{12} + 2k_{BP}A_{11}T_{11}^{\ 2} + 2k_{BP}A_{11}^{\ 3}T_{12}^{\ 2} + k_{BP}^{\ 2}A_{11}^{\ 2}T_{11}T_{12} - 4A_{11}^{\ 2}T_{11}T_{12}\right)\left(T_{11} + A_{11}T_{12}\right)}{4A_{11}T_{11}T_{12} + 2T_{11}^{\ 2} + 2A_{11}^{\ 2}T_{12}^{\ 2} + k_{BP}A_{11}T_{11}T_{12}} \tag{20}$$

$$e_1 = c_2 = A_{11}^{\ 2} \tag{21}$$

#	Op-amp Specifications			Desired Center Frequency, f_n	Actual Center Frequency	H_{BP}	Pole Locations from HSPICE
	A_0	BW	GBP				
1	200 kV/V	2.5 kHz	500 MHz	28 MHz	27 MHz	4.4k	(0.002 ± j26) MHz (-528 ± j26) MHz
2	200 kV/V	5 kHz	1 GHz	28 MHz	27 MHz	40	(-0.641 ± j27) MHz (-1030 ± j27) MHz
3	200 kV/V	12.5 kHz	2.5 GHz	28 MHz	28 MHz	24	(-1080 ± j28) MHz (-2530 ± j28) MHz
4	200 kV/V	25 kHz	5 GHz	28 MHz	28 MHz	21	(-1240 ± j28) MHz (-5030 ± j28) MHz
5	200 kV/V	5 kHz	1 GHz	56 MHz	53 MHz	4.1k	(0.005 ± j53) MHz (-1060 ± j53) MHz
6	2 MV/V	2.5 kHz	5 GHz	280 MHz	264 MHz	4.5k	(0.024 ± j265) MHz (-5280 ± j265) MHz

Table 1. State variable filter instability conditions using op-amp integrators

IV. OTA-C realization

Since the op-amp integrator is a closed-loop architecture, the op-amp itself must be compensated to ensure a dominant-pole open-loop frequency response. This narrow-banding reduces the GBP, and therefore, reduces the frequencies at which the op-amp integrator can be operated. The OTA, however, remains an open-loop configuration and achieves integration by capacitive output termination. This open-loop topology helps to give the OTA-C a superior frequency response to that of the op-amp integrator. Fig. 5 shows a model of an OTA-C integrator where g_{m2} is the transconductance of the amplifier, R_{OUT} is the amplifier output resistance, and C_{INT} is the integrating capacitor. The sub-circuit of g_{m1}, R_{POLE}, and C_{POLE}, creates a dominant pole to simulate the frequency response of the actual amplifier.

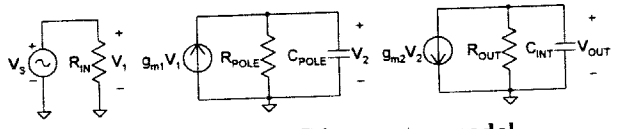

Figure 5. OTA-C integrator model

A. Theoretical analysis

Replacing each integrator in the filter of Fig. 2 with the model of Fig. 5 again results in a fourth-order circuit. This filter is shown in Fig. 6.

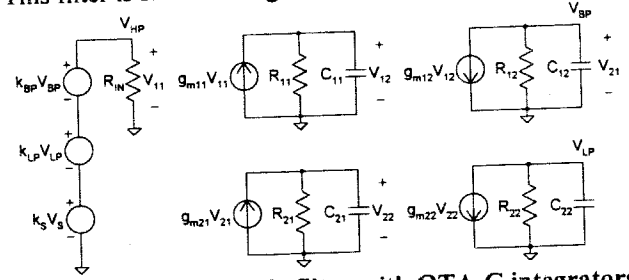

Figure 6. State variable filter with OTA-C integrators

The bandpass transfer function is

$$\frac{V_{BP}}{V_S} = \frac{k_S X_{21}}{X_{11}X_{21} - k_{LP}A_{11}A_{12}A_{21}A_{22} + k_{BP}X_{21}} \tag{24}$$

where

$$X_{11} = 1 + s(T_{11} + T_{12}) + s^2 T_{11}T_{12} \tag{25}$$

$$X_{21} = 1 + s(T_{21} + T_{22}) + s^2 T_{21}T_{22} \tag{26}$$

and $T_{ij} = R_{ij}C_{ij}$, $A_{ij} = g_{mij}R_{ij}$, for $i = 1, 2$ and $j = 1, 2$.

Simplifying (24) with $g_{m11} = 1/R_{11}$ and $g_{m21} = 1/R_{21}$, the bandwidth of the OTA and center frequency of the filter are

$$BW = \frac{1}{R_{POLE}C_{POLE}} \tag{27}$$

where $R_{POLE} = R_{11} = R_{21}$ and $C_{POLE} = C_{11} = C_{21}$, and

$$\omega_n = \frac{g_m\sqrt{-k_{LP}}}{C_{\omega n}} \tag{28}$$

where $g_m = g_{m12} = g_{m22}$ and $C_{\omega n} = C_{12} = C_{22}$.

Repeating the stability analysis used for the op-amp implementation, the Routh-Hurwitz criterion is once again applied. Before simplifying the denominator of (24), assumptions concerning the relative values of the circuit parameters need to be made. Typical values selected for the transconductance (g_m), bandwidth, and output resistance ($R_{OUT} = R_{12} = R_{22}$) of the OTA are g_m = 15 mmhos, BW = 700 MHz, and R_{OUT} = 75 kΩ. Using typical values of Q, the four assumptions, $g_mR_{OUT} >> Q$, $g_mR_{OUT} >> 1/Q$, $g_mR_{OUT} >> 1$, and $g_mR_{OUT}BW >> \omega_n$ are easily satisfied.

With the proper assumptions, and again assuming the two integrators are matched such that that $A_{11} = A_{21}$, $T_{11} = T_{21}$, and $T_{12} = T_{22}$, the characteristic polynomial of (24) has the same form as (11), where

$$a_4 = T_{11}^{\ 2} T_{12}^{\ 2} \tag{29}$$

$$a_3 = 2T_{11} T_{12}^{\ 2} \tag{30}$$

$$a_2 = T_{12}\left(T_{12} + k_{BP} A_{12} T_{11}\right) \tag{31}$$

$$a_1 = k_{BP} A_{12} T_{12} \tag{32}$$

$$a_0 = A_{12}^{\ 2} \tag{33}$$

The fourth-order Routhian array has the same form as (17), and the remaining array elements can be calculated from (18) through (21) to be

$$c_1 = \frac{2T_{12}^{\ 2} + k_{BP} A_{12} T_{11} T_{12}}{2} \tag{34}$$

$$c_2 = A_{12}^{\ 2} \tag{35}$$

$$d_1 = \frac{\left(2T_{12} + k_{BP} A_{12} T_{11}\right) k_{BP} A_{12} T_{12} - 4A_{12}^{\ 2} T_{11} T_{12}}{2T_{12} + k_{BP} A_{12} T_{11}} \tag{36}$$

$$e_1 = A_{12}^{\ 2} \tag{37}$$

Again, Routhian array first column elements a_4, a_3, c_1, and e_1 are positive, so stability is ensured if d_1 is also positive. Element d_1 is positive for

$$\frac{2BW}{\omega_n} > 4Q - \frac{1}{Q} \tag{38}$$

For Q > 2, (38) may be approximated as

$$BW > 2Q\omega_n \tag{39}$$

B. Simulation results

The inequality of (39) is also derived in [7] using a simplified analysis which requires $Q > 1$. Although (38) reduces to (39) for moderate values of Q, (38) is far more accurate for $Q < 1$. At $Q = 0.5$, for example, (38) correctly predicts the filter will be stable at all frequencies, while (39) predicts instability for $\omega_n > BW$. HSPICE simulations verify the accuracy of both (38) and (39), however, as (39) may be used for most filters, it will be used to present simulation results.

To ensure stability, (39) indicates that the bandwidth, BW, of the OTAs used in the state variable filter of Fig. 1 must be at least twice the product of the quality factor, Q, and the desired center frequency, ω_n. Similar to the op-amp implementation, moving the poles farther from the imaginary axis to eliminate peaking at the center frequency requires the BW of the OTAs to be even larger – typically 10 times larger – than $2Q\omega_n$. HSPICE simulations verify this claim, as indicated by the results in Table 2. As in the previous case, Q and H_{BP} are designed to be 10 and 19, respectively, for all simulations. Since $Q > 2$, (39) may be used to predict stability.

In the first simulation of Table 2, (39) is not satisfied with the selected values of Q, ω_n, and BW. As in the first simulation in the op-amp analysis, the filter is unstable and has poles in the right-half of the complex frequency plane. The next three simulations use an increasingly larger BW, and the resulting H_{BP} decreases as the poles move into the left-half plane and farther from the imaginary axis. The last simulation doubles the BW from 700 MHz to 1.4 GHz, causing the frequency of oscillation to double from 36 to 72 MHz. The stability of the OTA-C integrator filter, therefore, behaves exactly as (39) predicts.

#	OTA BW	Desired Center Frequency, f_n	Actual Center Frequency	H_{BP}	Pole Locations from HSPICE
1	700 MHz	36 MHz	36 MHz	1 k	(0.033 ± *j*36) MHz (-701 ± *j*36) MHz
2	1.4 GHz	36 MHz	36 MHz	39	(-0.887 ± *j*36) MHz (-1400 ± *j*36) MHz
3	3.5 GHz	36 MHz	36 MHz	24	(-1.44 ± *j*36) MHz (-3500 ± *j*36) MHz
4	7 GHz	36 MHz	36 MHz	21	(-1.63 ± *j*36) MHz (-7000 ± *j*36) MHz
5	1.4 GHz	72 MHz	72 MHz	883	(0.076 ± *j*72) MHz (-1400 ± *j*72) MHz

Table 2. State variable filter instability conditions using OTA-C integrators

V. Conclusion

The Routh-Hurwitz criterion is used to accurately assess the stability of a continuous-time state variable filter implemented with op-amp and OTA-C integrators. The resulting inequalities governing the stability of the two fourth-order transfer functions are similar. The results of the Routh-Hurwitz analyses indicate that the *GBP* of the op-amps, and the *BW* of the OTAs need to be very large if the filters comprising them are to be stable at the high frequencies used in state of the art communications circuits.

Acknowledgments

The authors would like to thank Edgar Sánchez-Sinencio and Mohammed Ismail for their constructive comments.

References

[1] L. P. Huelsman and P. E. Allen, *Introduction to the Theory and Design of Active Filters*. New York: McGraw-Hill Inc., 1980.

[2] C. Toumazou, F. J. Lidgey, and D. G. Haigh (eds.), *Analogue IC Design: The Current-Mode Approach*. London: Peter Peregrinus Ltd., 1990.

[3] R. L. Geiger and E. Sánchez-Sinencio, "Active Filter Design using Operational Transconductance Amplifiers: A Tutorial," *IEEE Circuits and Devices Magazine*, vol. 1, pp. 20-32, Mar. 1985.

[4] E. Sánchez-Sinencio, R. L. Geiger, and H. Nevárez-Lozano, "Generation of Continuous-Time Two Integrator Loop OTA Filter Structures," *IEEE Trans. Circuits and Systems*, vol. 35, pp. 936-946, Aug. 1988.

[5] Y. Sun and J. K. Fidler, "Structure Generation and Design of Multiple Loop Feedback OTA-Grounded Capacitor Filters," *IEEE Trans. Circuits and Systems*, Part I, vol. 44, pp. 1-11, Jan. 1997.

[6] J. Choma Jr., *Electrical Networks: Theory and Analysis*. New York: John Wiley and Sons, Inc., 1985.

[7] J. Ramírez-Angulo and E. Sánchez-Sinencio, "Active Compensation of Operational Transconductance Amplifier Filters using Partial Positive Feedback," *IEEE J. Solid-State Circuits*, vol. 25, pp. 1024-1028, Aug. 1990.